JOURNAL OF MATERIALS SCIENCE 19 (1984) 2969–2979

Influence of temperature and stress-relieving treatment of the stress relaxation in bending of Zircaloy-4 near 673 K

F. POVOLO
Comisión Nacional de Energía Atómica, Dto. de Materiales. Av. del Libertador 8250, (1429) Buenos Aires, Argentina, and Comisión de Investigaciones Científicas de la Provincia de Buenos Aires, La Plata, Argentina

J. C. CAPITANI
Comisión de Investigaciones Científicas de la Provincia de Buenos Aires, La Plata, Argentina

Stress relaxation data in bending and at 633 and 673 K, for stress-relieved, cold-worked and annealed Zircaloy-4, are reported. The data can be described by a creep model that involves jog–drag and cell-formation and the ratio of cell diameter to dislocation spacing, obtained from the stress relaxation curves, is shown to be dependent on the thermo-mechanical treatment given to the specimens, prior to the stress relaxation tests. Finally, the values $H_v \approx 87\,\text{kJ mol}^{-1}$ and $D_0 \approx 3.3 \times 10^{-15}\,\text{m}^2\,\text{sec}^{-1}$, for the activation enthalpy and the pre-exponential factor for self-diffusion, respectively, were obtained from the stress relaxation curves measured at the two temperatures.

1. Introduction

The 673 K creep behaviour of Zircaloy has recently become interesting for two reasons. With current nuclear fuel pin designs and power levels, the cladding inner diameter can achieve operating temperatures as high as 673 K. Secondly, the creep strain of Zircaloy at 240 h, 673 K, and 150 MPa is used as a quality control test for creep strength in Zircaloy clad. The available data show that the creep strength of Zircaloy-4*, for example, is strongly dependent on metallurgical structure (cold-work and annealing), texture and composition [1–4] but, the fundamental mechanisms controlling the creep of this alloy at 673 K are not well established.

Creep experiments with broad changes in the metallurgical structure are costly and time consuming, so that efforts have been made to obtain information about the creep behaviour from stress relaxation measurements. Huang *et al.* [5] have performed load relaxation tests as a function of temperature on Zircaloy-4 tubing with the applied stress in the direction of the tube axis. The experimental data were analysed using the approach of a plastic equation of state as proposed by Hart [6, 7] and the authors concluded that: (1) in the temperature range 473 to 658 K the results can be represented by the phenomenological model based on Hart's plastic equation of state; (2) at higher temperatures the load relaxation data suggest the contribution of grain-boundary sliding; (3) at temperatures near 673 K the tensile data suggest that the effects of strain ageing are not important.

Povolo and Higa [8] have reported stress relaxation measurements in bending, performed in Zircaloy-4 at 673 K up to times of the order of 1000 h, in stress-relieved and cold-worked specimens. The stress relieving treatments were

*Nominal composition (wt %): Sn (1.43), Fe (0.21), Cr (0.1), Zr (balance)

0022–2461/84 $03.00 + .12

made at three different temperatures: 773, 793 and 813 K, for 1 and 2 h. Contrary to the load relaxation data on tubing reported by Huang *et al.* at a similar temperature, it was found that the individual stress relaxation curves, taken at different initial stresses, could be related by scaling [6]. In fact, it was possible to superpose by translation any one of the curves on to any of the others in such a way that the overlapping segments of each curve match within experimental error. All the stress-relieved specimens showed the same scaling behaviour, but the cold-worked specimens gave a translation path of a different slope. The results were interpreted in terms of Hart's phenomenological model of plastic deformation, for high homologous temperatures and it was suggested that the stress relaxation is mainly controlled by grain-boundary sliding. Povolo and Marzocca [9, 10], however, have shown that the creep and stress relaxation data, taken at 673 K in cold-worked Zircaloy-4, may also be described by a model based on the diffusion controlled motion of jogged screw dislocations, proposed by Barrett and Nix [11]. Furthermore, an interrelation between the parameters of Hart's phenomenological equation for high homologous temperatures and those for the Barrett–Nix equation was established [12].

Keusseyan *et al.* [13], performed load relaxation tests on Zircaloy-2 and Zircaloy-4 sheets with various textures and microstructures, to study the influence of fabrication variables on the mechanical behaviour of these alloys. The data obtained primarily at temperatures (573 to 673 K) typical of cladding operating conditions, were interpreted in terms of Hart's phenomenological model for plastic deformation. The load relaxation curves obtained for the different materials were qualitatively similar with the exception of those obtained for 0° texture material. This material showed the lowest yield strength and no evidence for grain-boundary sliding at temperatures up to 573 K. According to the authors, the stress relaxation curves at 673 K were influenced by grain-boundary sliding.

More recently, Povolo and Peszkin [14] have reported stress relaxation data in bending in Zircaloy-4 with different degrees of cold work. The measurements were extended up to times of the order of 1000 h, with six different initial stresses. It was demonstrated that the stress relaxation curves, for a given thermomechanical treatment, are related by scaling and the slope of the translation path depends on the treatment given to the specimens prior to the relaxation testing. The data were interpreted in terms of Gittus' [15] creep model which involves jog–drag and cell-formation. The average spacing between neighbouring jogs and the ratio of cell diameter to dislocation spacing were obtained from the stress relaxation curves. Povolo and Marzocca [16] interpreted the creep characteristics, at 673 K, of cold-worked and stress relieved Zircaloy-4 with the same model. Furthermore, by means of a grain-counting technique it was shown that grain-boundary sliding gives only a small contribution to the creep strain, for the stresses and strain rate considered.

It is the purpose of this paper to present data of the stress relaxation in bending, of cold-worked, stress-relieved and annealed Zircaloy-4. The measurements are performed both at 633 and 673 K to study the influence of the temperature on the parameters of the theoretical model which describes the stress relaxation curves.

2. Experimental procedure

The specimens were prepared from a Zircaloy-4 plate which was fabricated according to ASTM B 352-64 T standards. The as-received plate had the following dimensions: 6 mm thick, 15 mm wide and 1 m long, and the original rolling direction was along the largest dimension. The texture of this plate, as determined by the Schulz technique, is indicated by the (0 0 0 2) pole figure shown in Fig. 1. The chemical composition of the alloy is given in Table I.

Since specimens 1 mm thick were needed for the stress relaxation experiments, it was necessary to reduce the original plate by cold-rolling. The following procedure was used: the as-received plate was cut into parts and each part cold-rolled 20% thickness, along the original rolling direction. Then they were annealed at 1073 K, for 1 h in a high vacuum, and cold-rolled again to the same percentage and in the same direction. The sequence was repeated, except for the last rolling, where a 50% reduction in thickness was used. The 20% reduction (except during the last rolling) between annealing treatments, was mantained to avoid cracking of the material. The samples for the stress relaxation experiments were machined from this material, with the axis parallel to the rolling direction, with dimensions 1 mm thick, 10 mm

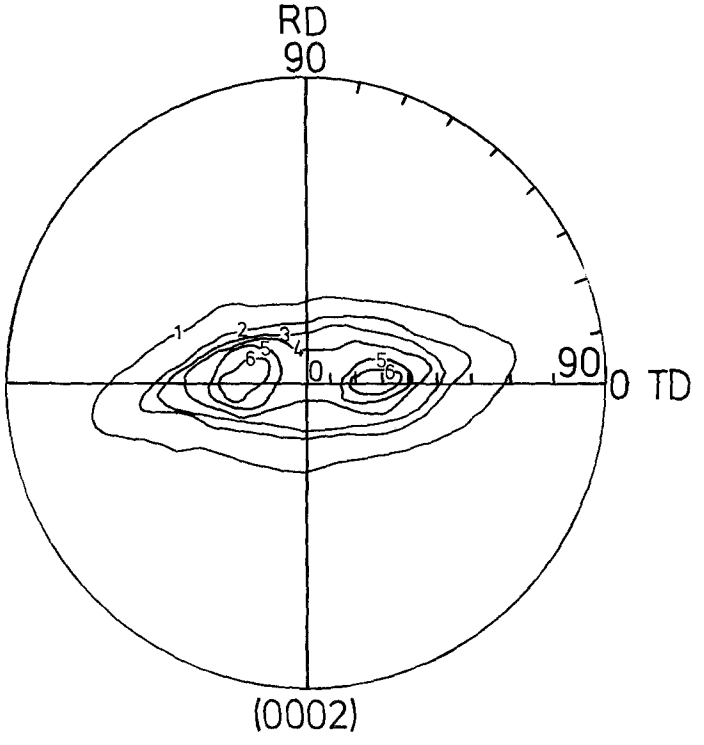

Figure 1 (0 0 0 2) pole figure for the as-received Zircaloy-4 plate.

wide and 100 mm long. The texture of these specimens is shown in Fig. 2.

Different thermal treatments, in vacuum, were given to the specimens prior to the stress relaxation experiments. These treatments are named A, B, C and D, respectively, as indicated in Table II. The pole figures after treatments B and C are similar to the pole figure given in Fig. 2, since the material has only recovered and stress relieved. Annealing treatment D changes the pole figure to a distribution with a maximum intensity of basal poles located near the normal direction [14].

The specimens, originally flat, were bent elastically in stainless steel holders with radii which gave maximum outer fibre stresses, Σ, between 100 and 300 MPa, calculated from the expression

$$\Sigma = Eh/2R \quad (1)$$

where E is Young's modulus (100 GPa for Zircaloy-4 at room temperature [17]), R is the radius of the holder, and h the thickness of the specimen. The initial outer fibre stresses used are indicated in Table III.

Duplicate holders, similar to those described by Fraser *et al.* [18], were used to perform measurements at 633 and 673 K simultaneously. These holders were inserted into the corresponding furnace and extracted periodically for curvature

TABLE IA Composition of Zircaloy-4

Constituents	(%)
Sn	1.48
Fe	0.23
Cr	0.12
Fe + Cr	0.35

TABLE IB Main impurities (ppm)

Constituents	
C	112
Hf	62
N	51
W	< 50
Si	44
O	980

TABLE II Thermomechanical treatment given to the specimens prior to the stress relaxation tests

Thermomechanical treatment	Name
50% cold-rolled	A
A + 1 h at 813 K	B
A + 2 h at 813 K	C
A + 3 h at 1023 K	D

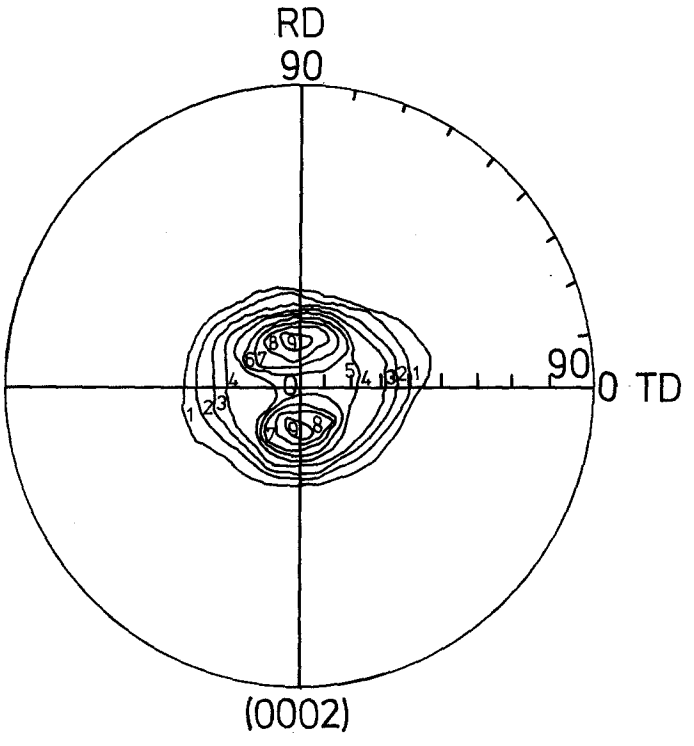

Figure 2 (0 0 0 2) pole figure for the 50% cold-rolled type-A specimens.

measurements. The temperature was controlled with thermocouples attached to the holders near the specimens and the fluctuations were of the order of ± 1 K; the accumulated time for relaxation was of the order of 1000 h.

The radii of curvature, R_i, after releasing the specimens from the holders were determined in the way described in [8]. Duplicate specimens were used in order to observe the dispersion between equivalent specimens on the results. The measured stress change at the surface of the bent specimen, σ_b, after releasing it from the holder, is given by

$$\sigma_b = (Eh/2)(1/R - 1/R_i) \quad (2)$$

where $E = 72.6$ GPa at 673 K and $E = 74.86$ GPa at 633 K [17]. The stress at the surface of the beam before unloading, σ, can be obtained from the relationship [19, 20]

$$\sigma = \frac{2}{3}\sigma_b + \frac{\Sigma}{3}(d\sigma_b/d\Sigma) \quad (3)$$

TABLE III Initial stresses at the surface of the bent specimens (MPa)

Σ_1	115.6
Σ_2	204.4
Σ_3	306.8

with Σ given by Equation 1 and σ_b by Equation 2. σ is an equivalent uniaxial stress and represents the stress that would be obtained at the surface of the beam under an initial uniaxial stress given by Σ.

3. Results

Figs. 3 to 5 show the measured stress change at the surface of the specimens, σ_b (Equation 2), as a function of time, both at 633 and 673 K, for the specimens with different thermomechanical treatments and the three initial stresses. The data points represent the average values obtained in two similar specimens. In this paper A, B, C, D will indicate specimens with the thermomechanical treatments given in Table I tested at 633 K, and A′, B′, C′, D′ specimens with the same thermomechanical treatments but tested at 673 K.

The stresses, σ, at the surface of the specimens before unloading, which correspond to the values that would be obtained in the same material, under initial uniaxial stresses given by Σ, can be calculated using Equation 3 and the procedure described in [19]. These curves are not given to save space. The logσ–log$\dot{\varepsilon}$ stress relaxation curves, where $\dot{\varepsilon}$ is the plastic strain rate, are obtained by calculating the derivatives of the σ against t curves, since $\dot{\varepsilon} = -\dot{\sigma}/E$, where E is taken at the corre-

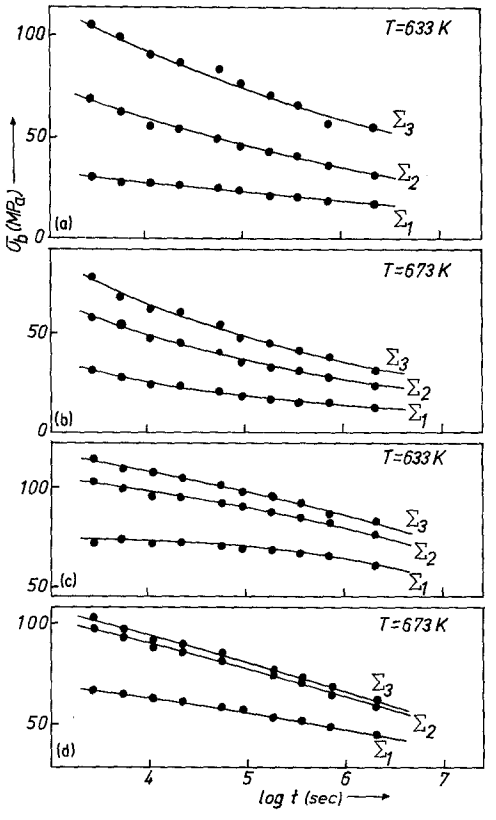

Figure 3 Measured stress change at the surface as a function of time. (a) type-A, (b) type-A′, (c) type-C and (d) type-D′ specimens.

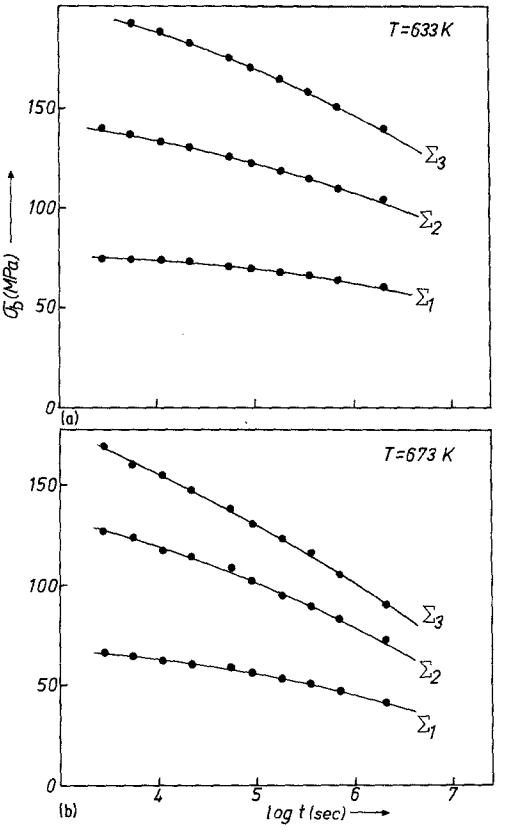

Figure 4 Measured stress change at the surface as a function of time. (a) type-B and (b) type-B′ specimens.

sponding temperature and the dot indicates a derivative with respect to the time. These curves are shown in Figs. 6 and 7. Two curves are obtained, in some cases, from the data measured at the intermediate initial stress. These two different curves result from the fact that Equation 3 can be applied to the σ_b–t curves either with $d\Sigma = \Sigma_3 - \Sigma_2$ or with $d\Sigma = \Sigma_2 - \Sigma_1$ [8]. The curve marked Σ_2 is obtained in the first case, and that marked Σ_2' in the second case.

The logσ–log$\dot{\epsilon}$ curves shown in Figs. 6 and 7 are related by scaling [6]. In fact, for specimens with a given thermomechanical treatment and at a given temperature, it is possible to superpose by translations ($\Delta\log\sigma$–$\Delta\log\dot{\epsilon}$) any one of the curves, at a given Σ, on to any of the others in such a way that the overlapping segments of each curve match within experimental error. The translation is made along the translation path of the slope

$$\mu = \Delta\log\sigma/\Delta\log\dot{\epsilon} = \text{constant} \qquad (4)$$

The master curves obtained by translating, for each type of specimen and at each temperature, all the curves on to the curve for Σ_1 are shown in Fig. 8. The corresponding translation paths are indicated by the straight lines and the slopes are given in Table IV. These slopes were obtained using a method to be described later in the paper.

4. Discussion

The individual curves of Figs. 6 and 7 and the master curves of Fig. 8 can be described analytically by the constitutive equation

$$\alpha\sigma = (\dot{\epsilon}/\dot{\epsilon}^*)^{1/3} + \sinh^{-1}[(\dot{\epsilon}/\dot{\epsilon}^*)^{1/3}\beta] \qquad (5)$$

where

$$\beta = G^2ABK^6; \qquad (6)$$

$$\dot{\epsilon}^* = B(kT)^3K^6/b^3l^3 \qquad (7)$$

$$\alpha = b^2l/kT; \qquad (8)$$

$$B = c_jD_vb/G^2kT; \qquad (9)$$

$$A = b^2/20\alpha D_v \qquad (10)$$

b is Burgers vector, G is the shear modulus, D_v is the volume self-diffusion coefficient, l is the distance between neighbouring jogs on dislo-

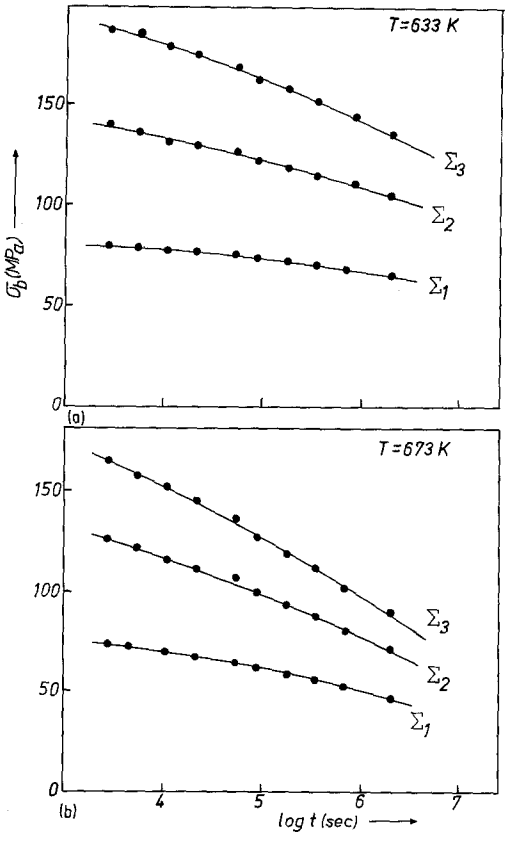

Figure 5 Measured stress change at the surface as a function of time. (a) type-C and (b) type-C' specimens.

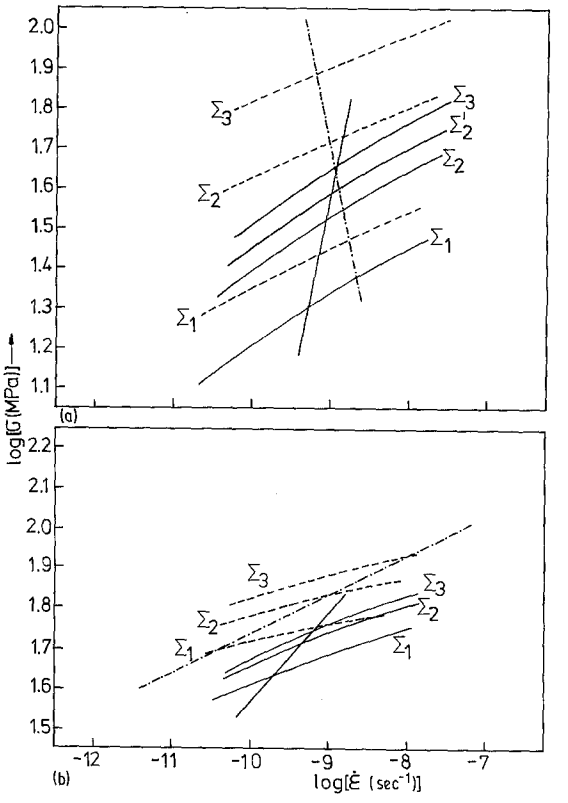

Figure 6 Stress against strain rate relaxation curves. (a) Broken curves type-A, full curves type-A'; (b) broken curves type-D, full curves type-D'. The straight lines indicate the translation paths.

cations, c_j is the thermal jogs concentration, K is the ratio of cell diameter to dislocation spacing, k is Boltzmann's constant and T the absolute temperature. Equation 5 was given by Gittus [15] and takes into account the effects of jog–drag and cell-formation upon the rate of creep. This equation is plotted in Fig. 9 as $\log(\alpha\sigma)$ against $\log(\dot{\epsilon}/\dot{\epsilon}^*)$, for different values of β. Since Figs 8 (or Figs. 6 and 7) and 9 are plotted in the same scales, by superimposing both figures and translating along the axes (without rotations) [21] it is easily seen that the master curves of Fig. 8 can be matched to some curves of Fig. 9. The parameters α and $\dot{\epsilon}^*$ can be obtained from the coincidence of some value of $\log\sigma$ and $\log\dot{\epsilon}$ from the experimental curve with the corresponding $\log(\alpha\sigma)$ and $\log(\dot{\epsilon}/\dot{\epsilon}^*)$ values from the theoretical ones. β is read directly. Equation 5 was deduced by Gittus under steady-state conditions but Povolo and Marzocca [16] have shown that this equation may also be valid during transient creep. When the master curves of Fig. 8 are superimposed on the normalized plot of Equation 5, given in Fig. 9, to obtain the parameters α, $\dot{\epsilon}^*$ and β, it is implicitly assumed that β is constant for all the individual curves of Figs. 6 and 7, corresponding to a given thermomechanical treatment. On taking into account the scaling conditions for Equation 5 [22, 23] it can be shown that $\mu = 1/2$ if β is the same for all the individual curves, for a given treatment and at a given temperature. As shown in Table IV, however, the experimental values for the slopes of the translation paths are different from 1/2, which means either that the data cannot be described by Equation 5 or that β is variable. In fact, as shown by Povolo *et al.* [14, 23] when $\sinh^{-1}[\beta(\dot{\epsilon}/\dot{\epsilon}^*)^{1/3}] \gg (\dot{\epsilon}/\dot{\epsilon}^*)^{1/3}$ and $\sinh(\alpha\sigma) \approx \frac{1}{2}\exp(\alpha\sigma)$, Equation 5 reduces to

$$(\dot{\epsilon}/\dot{\epsilon}^*) = (1/8\beta^3)\exp(3\alpha\sigma). \qquad (11)$$

Equation 11, which is a limiting form of Equation 5, can lead to a scaling behaviour with variable β in a log–log diagram and the scaling conditions are

$$\Delta\log\alpha = -\mu\Delta\log\dot{\epsilon} \qquad (12)$$

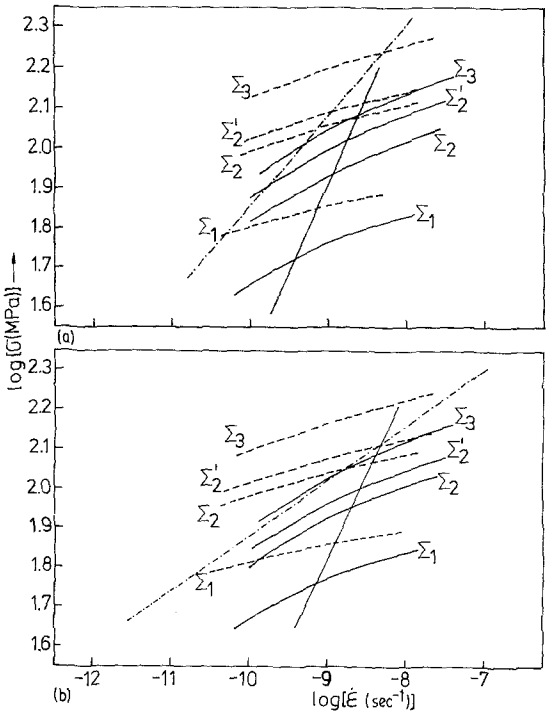

Figure 7 Stress against strain rate relaxation curves. (a) Broken curves type-B, full curves type-B'; (b) broken curves type-C, full curves type-C'. The straight lines indicate the translation paths.

$$\Delta\log\dot{\epsilon}^* = (3\mu - \tfrac{1}{2})\Delta\log\dot{\epsilon} \qquad (13)$$

$$\Delta\log\beta = (\mu - \tfrac{1}{2})\Delta\log\dot{\epsilon} \qquad (14)$$

These equations lead to $\Delta\log\beta = 0$ for $\mu = \frac{1}{2}$.

It is difficult to obtain the parameters of the individual curves shown in Figs. 6 and 7, by superimposing them to the normalized plot of Equation 5 since they are too short and the parameters cannot be unambiguously determined. A similar situation is found for the master curves of Fig. 8 since the experimental range is extended only slightly. If Equation 5 reduces to Equation 11, then a plot of the data of Figs. 6 and 7 as $\ln\dot{\epsilon}$ against σ, at different initial stresses, gives straight lines of slope 3α and intercept $\dot{\epsilon}^*/8\beta^3$. Furthermore, on combining Equations 12 to 14 it is easy to show that

$$\dot{\epsilon}^*/\beta^3 = C_1(\alpha)^{-1/\mu} \qquad (15)$$

where C_1 is a constant for a given thermomechanical treatment and at a given temperature. The data of Figs. 6 and 7 give straight lines when plotted as $\ln\dot{\epsilon}$ against σ. In addition, as suggested by Equation 15, a plot of $\log(\dot{\epsilon}^*/\beta^3)$ against $\log\alpha$ should give a straight line of slope $-1/\mu$. This last plot allows a determination of the slope of the translation path very accurately. The values given in Table IV were determined in this way.

TABLE IV Slopes of the translation paths shown in Fig. 8

Specimen type	μ
A	−0.96
A'	1.00
B	0.23
B'	0.45
C	0.14
C'	0.43
D	0.10
D'	0.23

From Equations 6 to 10 it is easy to show that

$$\beta = G^2b^2\alpha^2\dot{\epsilon}^*/20D_v \qquad (16)$$

so that once α and $\dot{\epsilon}^*/\beta^3$ are known, $\dot{\epsilon}^*$ and β can be calculated using Equation 16. The problem is that Equation 16 involves D_v and there is some disagreement in the literature about the self-diffusion coefficient for zirconium [24], which can give differences of various orders of magnitude between the self-diffusion coefficients extra-

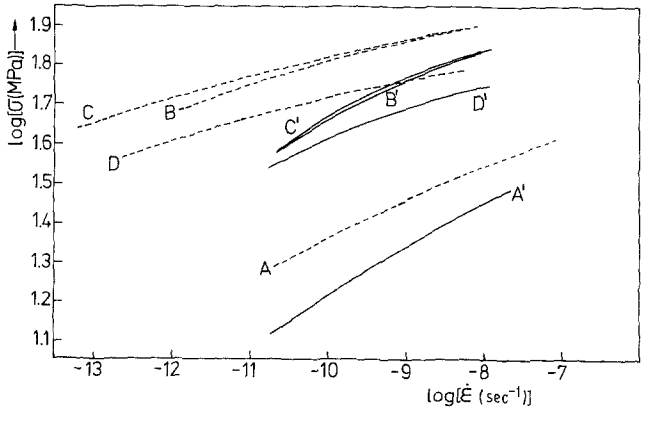

Figure 8 Master curves obtained by translating the individual curves of Figs. 6 and 7 on to the curves for Σ_1, along the translation paths indicated in the same figures.

polated to temperatures of the order of 673 K. In this situation the following procedure was preferred: α is determined, for each of the master curves of Fig. 8, from the linear plots of $\ln \dot{e}$ against α, as suggested by Equation 11. Once α is known, for each type of specimen, the procedure of superimposing Fig. 8 on Fig. 9 can be done only by a translation parallel to the $\log(\dot{e}/\dot{e}^*)$ axis, reducing the error in the determination of $\dot{e}^*$ and β. Equation 16 can now be used to calculate D_v, with $G = 26\,\text{GPa}$ at 673 K, $G = 27\,\text{GPa}$ at 633 K [17] and $b = 3.23 \times 10^{-10}\,\text{m}$, leading to the average values for the self-diffusion coefficients at the two temperatures

$$D_v = 2.0 \times 10^{-22}\,\text{m}^2\,\text{sec}^{-1} \text{ at } 633\,\text{K} \quad (17)$$

$$D_v = 5.3 \times 10^{-22}\,\text{m}^2\,\text{sec}^{-1} \text{ at } 673\,\text{K} \quad (18)$$

These are average values since the procedure described gives slightly different self-diffusion coefficients for specimens with different thermomechanical treatments. These different coefficients result from the fact that Equation 5 is used in polycrystals with different average orientation factors.

On taking into account that $D_v = D_0 \exp(-H_v/kT)$ where H_v is the activation enthalpy for self-diffusion, Equations 17 and 18 give

$$H_v \approx 87\,\text{kJ mol}^{-1} \quad (19)$$

$$D_0 \approx 3.3 \times 10^{-15}\,\text{m}^2\,\text{sec}^{-1} \quad (20)$$

These values seem to be confirmed by recent measurements of the self-diffusion coefficient using ion-beam-sputtering techniques [25]. Furthermore, recent creep data at 673 K, in cold-worked and stress-relieved Zircaloy-4 lead to a self-diffusion coefficient similar to the value given by Equation 18 [16]. It must be pointed out that D_0 can be affected by a large error since, for example, on increasing H_v by 20% D_0 changes to values of the order of 10^{-13}.

The parameters for the master curves of Fig. 8 coincide with those of the individual curves for Σ_1, shown in Figs. 6 and 7. Once the parameters for one of the individual curves are known, those for the rest of the individual curves can be obtained by using, for a given type of specimen and at a given temperature, the translation conditions given by Equations 12 to 14. In fact, once α, $\dot{\epsilon}^*$ and β are known for one of the individual curves, since the increments $\Delta\log\dot{\epsilon}$, needed to translate the individual curves, can be easily determined, Equations 12 to 14 can be used to calculate $\Delta\log\alpha$, $\Delta\log\dot{\epsilon}^*$ and $\Delta\log\beta$ and, consequently, to obtain the parameters for the rest of the individual curves from those of the reference curves. The detailed procedure is given elsewhere [23] but it should be pointed out that the curves of Figs. 6 and 7 can be fitted either with Equation 11 or with Equation 5 with a maximum error of the order of 2%.

The average distance between neighbouring jogs and the ratio of cell diameter to dislocation spacing can be obtained from α, $\dot{\epsilon}^*$ and β using Equations 6 to 10 and c_j given by [26]:

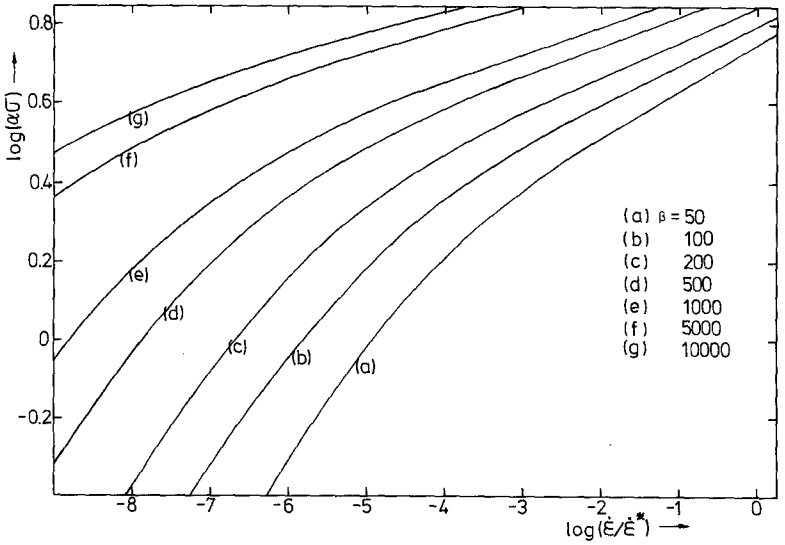

Figure 9 Normalized plot of Equation 5.

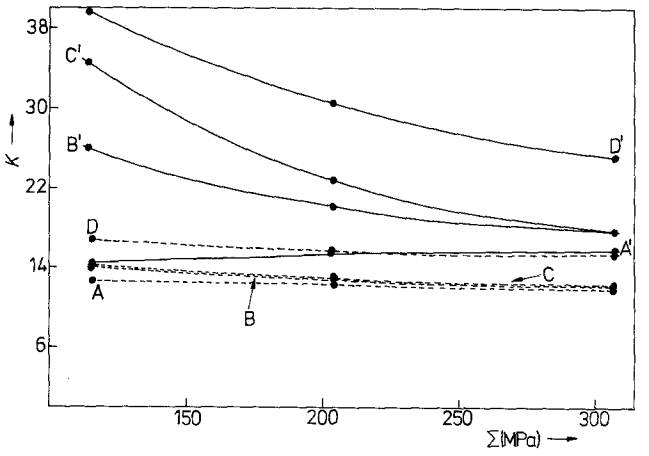

Figure 10 Ratio of cell diameter to dislocation spacing as a function of the initial maximum outer fibre stress, for the different specimens and the two temperatures.

$$c_j = \exp(-xGb^3/kT) \qquad (21)$$

$$0.2 > x \geqslant 1/8\pi$$

On taking $x = 1/8\pi$ this equation leads to $c_j = 2.35 \times 10^{-2}$ at 673 K, $c_j = 1.59 \times 10^{-2}$ at 633 K. The ratio of cell diameter to dislocation spacing, K, is shown in Fig. 10 as a function of the initial maximum outer fibre stress, for the different specimens and at the two temperatures. The average distance between neighbouring jogs, l, in units of the Burgers vector is shown in Fig. 11 as a function of the reciprocal of the initial maximum outer fibre stress, for the different specimens and at the two temperature. It is seen that l changes linearly with $1/\Sigma$.

According to Fig. 10, K remains practically constant for all the specimens at 633 K. At 673 K, K is practically independent of Σ for the cold-worked specimens and decreases with the initial stress for annealed and stress-relieved specimens. This behaviour is similar to that found for specimens with different degrees of cold-work, reported by Povolo and Peszkin [14] for the stress relaxation in bending of Zircaloy-4 at 673 K. In fact, it was found that K did not change with Σ as cold-work increased and the strongest variation was obtained for annealed specimens. The dependence of K with Σ reflects the fact that the initial stress changes the dislocation structure and, as expected, the influence is stronger as the temperature increases but diminishes as cold-work increases.

The values of K shown in Fig. 10 are of the order of magnitude of those obtained by observations of the microstructure in several metals and alloys [27] and lie in the range predicted theoretically by Gittus [28], i.e. $20 > K > 5$. The experimental values for specimens B', C' and D' are slightly high but it should be pointed out that the measurements have been performed in polycrystals and Equation 5 is strictly valid for single crystals. In addition, several assumptions were made by Gittus during his theoretical calculations for K.

It is interesting to discuss the significance of the slope of the translation path. In fact, as shown in Table IV, μ depends on the thermomechanical treatment and on temperature. Povolo and Peszkin also observed that the slope of the translation path depended strongly on the thermomechanical treatment. Combining Equations 12 to 14 leads to

$$\dot{\epsilon}^* = C\alpha^{(1/2\mu-3)} \qquad (22)$$

where C is a constant at a given temperature and for a given thermomechanical treatment. Taking into account the definition of $\dot{\epsilon}^*$ and α, as given by Equations 7 and 8, and Equation 9 give

$$K^6 = (CG^2/c_j D_v)b^{(1/\mu-4)}(kT)^{(1-1/2\mu)}l^{1/2\mu} \qquad (23)$$

If, as assumed by Gittus, l is related to c_j by

$$l = b/c_j \qquad (24)$$

then, Equation 23 can be written as

$$K = (CG^2/D_v)^{1/6} b^{(3/2\mu-4)}(kT)^{(1-1/2\mu)} \times c_j - (1/6 + 1/12\mu) \qquad (25)$$

since the stress relaxation curves are related by scaling and K and l are not independent, as shown by Equation 23. Furthermore, if c_j is related to l through Equation 24 then, as shown by Equation 25, $\log K$ changes linearly with $\log c_j$ and both the

slope and the intercept depend on μ. Gittus [28] has deduced a theoretical relationship between K and c_j, showing that $\log K$ is linearly related to $\log c_j$. The approximate solutions of the theoretical equation are

$$K \approx (0.03c')^{-1/12} c_j^{-1/3} \quad (26)$$

and

$$K \approx 1.58 c_j^{-0.4} \quad (27)$$

valid for finite values of c' and $K > 5$ and, for $c' = 0$ and $K \geqslant 1$, respectively. c' is defined by $c'K^2 = (G - G_r)/G_r$ where G_r is the shear relaxed modulus. The approximate Equations 26 and 27 show that the slope of the plot of $\log K$ against $\log c_j$ is negative.

From Equation 25 and the values for μ reported in Table IV it can be seen that the experimental slopes change between approximately -0.1 and -0.25, depending on the thermomechanical treatment and temperature. Furthermore, the intercepts also depend on temperature and on the previous history of the material.

Equations 26 and 27 were obtained by Gittus by taking a limiting form of Equation 5 and by making several additional assumptions and they should be considered only as approximate. In fact, as shown by Equation 23, K depends on l through a power law, and on using Equation 24 it is implicitly assumed that only thermal jogs are present. This is not strictly valid since, as shown by Fig. 11, l depends also on Σ. A detailed discussion on the theoretical value of K is given elsewhere [29]. Finally, it should be pointed out that creep data, at 673 K, for cold-worked and stress-relieved Zircaloy-4 could be interpreted by using the same model. Values of K in the range 20 to 5 were obtained and stress-relieved specimens showed higher values of K as compared with the cold-worked ones.

5. Conclusions

The stress relaxation in bending, at 633 and 673 K, of cold-worked, stress-relieved and annealed Zircaloy-4 can be very well described by a creep model that involves jog–drag and cell-formation. The ratio of cell-diameter to dislocation spacing, obtained from the stress relaxation curves, was shown to be dependent on the thermomechanical treatment given to the specimens, prior to the stress relaxation tests.

Finally, the activation enthalpy and the pre-exponential factor for the self-diffusion of zirconium could be obtained from the stress relaxation curves measured at the two temperatures.

Acknowledgements

This work was performed within the Special Intergovernmental Agreement between Argentina and the Federal Republic of Germany and was supported in part by the "Proyecto Multinacional de Tecnología de Materiales" OAS-CNEA and the CIC.

References

1. K. KÄLLSTRÖM, T. ANDERSSON and A. HOFVENSTAM, Zirconium in Nuclear Applications, ASTM STP 551 (American Society for Testing and Materials, Philadelphia, 1974) p. 160.
2. K. KÄLLSTRÖM, *Scand. J. Met.* **4** (1975) 65.
3. V. FIDLERIS, *Atomic Energy Rev.* **13** (1975) 51.
4. G. E. LUCAS, thesis, MIT (1978).
5. F. H. HUANG, G. P. SABOL, S. G. McDONALD and CHE-YU LI, *J. Nucl. Mater.* **79** (1979) 214.

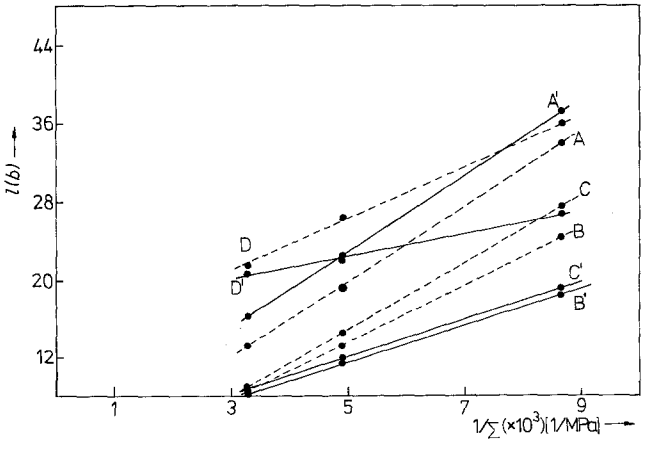

Figure 11 Distance between neighbouring jogs in units of the Burgers vector plotted against the reciprocal of the initial maximum outer fibre stress, for the different specimens and the two temperatures.

6. E. W. HART, CHE-YU LI, H. YAMADA and C. L. WIRE, "Constitutive Equations in Plasticity", edited by A. Argon (MIT Press, Cambridge, MA, 1975) p. 149.
7. E. W. HART, *J. Eng. Mat. Technol.* **98** (1976) 193.
8. F. POVOLO and M. HIGA, *J. Nucl. Mater.* **91** (1980) 189.
9. F. POVOLO and A. J. MARZOCCA, *ibid.* **97** (1981) 323.
10. *Idem, ibid.* **98** (1981) 322.
11. C. R. BARRETT and W. D. NIX, *Acta Metall.* **13** (1965) 1247.
12. F. POVOLO and A. J. MARZOCCA, *J. Nucl. Mater.* **99** (1981) 317.
13. R. L. KEUSSEYAN, J. WANAGEL, H. OCKEN, J. T. A. ROBERTS and CHE-YU LI, *ibid.* **98** (1981) 86.
14. F. POVOLO and P. N. PESZKIN, *Res. Mechanica* **6** (1983) 233.
15. J. H. GITTUS, *Phil. Mag.* **34** (1976) 401.
16. F. POVOLO and A. J. MARZOCCA, *J. Nucl. Mater.* **118** (1983) 224.
17. H. E. ROSINGER, I. G. RITCHIE and A. J. SHILLINGLAW, Atomic Energy of Canada Limited Report AECL-5231 (1975).
18. D. E. FRASER, P. A. ROSS-ROSS and A. R. CAUSEY, *J. Nucl. Mater.* **46** (1973) 81.
19. F. POVOLO and E. H. TOSCANO, *J. Nucl. Mater.* **74** (1978) 76.
20. *Idem, ibid.* **78** (1978) 217.
21. F. POVOLO, *ibid.* **96** (1981) 178.
22. F. POVOLO and A. J. MARZOCCA, *J. Mater. Sci.* **18** (1983) 1426.
23. F. POVOLO, A. J. MARZOCCA and G. H. RUBIOLO, *Res. Mechanica* (1984) in press.
24. F. DYMENT and C. LIBANATI, *J. Mater. Sci.* **3** (1968) 349.
25. F. DYMENT, private communication (1983).
26. J. FRIEDEL, "Dislocations" (Pergamon Press, London, 1964) p. 60.
27. S. TAKEUCHI and A. S. ARGON, *J. Mater. Sci.* **11** (1976) 1542.
28. J. H. GITTUS, *Phil. Mag.* **35** (1977) 293.
29. F. POVOLO, A. J. MARZOCCA and J. C. CAPITANI, *ibid.* **48** (1984) 759.

Received 30 March
and accepted 29 November 1983